ORIGINAL RESEARCH

# Alveolar Macrophage ABCG1 Deficiency Promotes Pulmonary Granulomatous Inflammation

Matthew McPeek[1], Anagha Malur[1], Debra A. Tokarz[2], Kvin Lertpiriyapong[3], Kymberly M. Gowdy[4], Gina Murray[5], Christopher J. Wingard[6], Michael B. Fessler[7], Barbara P. Barna[1], and Mary Jane Thomassen[1]

[1]Program in Lung Cell Biology and Translational Research, Division of Pulmonary, Critical Care and Sleep Medicine, [4]Department of Pharmacology and Toxicology, and [5]Department of Pathology, East Carolina University, Greenville, North Carolina; [2]Department of Population Health and Pathobiology, College of Veterinary Medicine, North Carolina State University, Raleigh, North Carolina; [3]Center of Comparative Medicine and Pathology, Memorial Sloan Kettering Cancer Center, New York, New York; [6]School of Movement and Rehabilitation Sciences, Physical Therapy Program, Bellarmine University, Louisville, Kentucky; and [7]Immunity, Inflammation, and Disease Laboratory, National Institute of Environmental Health Sciences, National Institutes of Health, Research Triangle Park, North Carolina

ORCID IDs: 0000-0002-1802-7346 (D.A.T.); 0000-0002-7227-0697 (K.M.G.); 0000-0002-8251-5678 (C.J.W.); 0000-0002-8262-8613 (M.B.F.); 0000-0003-1229-7668 (M.J.T.).

## Abstract

Pulmonary granuloma formation is a complex and poorly understood response to inhaled pathogens and particulate matter. To explore the mechanisms of pulmonary granuloma formation and maintenance, our laboratory has developed a multiwall carbon nanotube (MWCNT)-induced murine model of chronic granulomatous inflammation. We have demonstrated that the MWCNT model closely mimics pulmonary sarcoidosis pathophysiology, including the deficiency of alveolar macrophage ATP-binding cassette (ABC) lipid transporters ABCA1 and ABCG1. We hypothesized that deficiency of alveolar macrophage ABCA1 and ABCG1 would promote pulmonary granuloma formation and inflammation. To test this hypothesis, the effects of MWCNT instillation were evaluated in ABCA1, ABCG1, and ABCA1/ABCG1 myeloid-specific knockout (KO) mice. Histological examination revealed significantly larger pulmonary granulomas in ABCG1-KO and ABCA1/ABCG1 double-KO animals when compared with wild-type animals. Evaluation of BAL cells indicated increased expression of CCL2 and osteopontin, genes shown to be involved in the formation and maintenance of pulmonary granulomas. Single deficiency of alveolar macrophage ABCA1 did not affect MWCNT-induced granuloma formation or proinflammatory gene expression. These observations indicate that the deficiency of alveolar macrophage ABCG1 promotes pulmonary granulomatous inflammation and that this is augmented by additional deletion of ABCA1.

**Keywords:** pulmonary sarcoidosis; granuloma; alveolar macrophage; lipid transporters; carbon nanotubes

Sarcoidosis is a chronic inflammatory condition characterized by the presence of nonnecrotizing granulomas. Although any organ can be affected, the lungs and mediastinal lymph nodes are involved in more than 90% of clinical cases (1). Diagnosis is dependent on excluding the presence of infectious agents or previous exposure to materials known to produce granulomatous lesions. Although the etiology of sarcoidosis remains unclear, current understanding suggests the presence of a poorly soluble antigen in genetically susceptible individuals. Epidemiological studies have found an association between the incidence of sarcoidosis and exposure to wood-burning stoves, fireplaces, and certain occupations, such as firefighting (2–4). These environments contain particulate matter of respirable sizes, including carbon nanotubes.

Carbon nanotubes are produced as the byproducts of combustion or manufactured

(Received in original form November 8, 2018; accepted in final form March 7, 2019)

Supported by the National Institutes of Health (NIH) grant ES025191 (M.J.T.), the Intramural Research Program of the NIH, National Institute of Environmental Health Sciences (NIEHS) grant Z01 ES102005 (M.B.F.), North Carolina State University's Center for Human Health and the Environment through NIEHS grant P30ES025128, and NIH Instrumentation Grant 1S10OD021615-01.

Author Contributions: concept and design—M.M., A.M., B.P.B., and M.J.T.; acquisition of data—M.M., D.A.T., K.L., and K.M.G.; analysis and interpretation—M.M., A.M., D.A.T., K.L., K.M.G., G.M., C.J.W., M.B.F., B.P.B., and M.J.T.; drafting of the manuscript—M.M., A.M., and M.J.T.

Correspondence and requests for reprints should be addressed to Mary Jane Thomassen, Ph.D., Division of Pulmonary, Critical Care, and Sleep Medicine, 3E-149 Brody School of Medicine, East Carolina University, Greenville, NC 27834. E-mail: thomassenm@ecu.edu.

This article has a data supplement, which is accessible from this issue's table of contents at www.atsjournals.org.

Am J Respir Cell Mol Biol Vol 61, Iss 3, pp 332–340, Sep 2019

Originally Published in Press as DOI: 10.1165/rcmb.2018-0365OC on March 8, 2019
Internet address: www.atsjournals.org

for use in industrial processes. Carbon nanotubes may also have adverse implications for human health. Assessing the respiratory toxicology of carbon nanomaterials, Lam and colleagues (5) observed granuloma-like lesions in the lungs of exposed animals. These observations prompted our laboratory to investigate the use of multiwall carbon nanotubes (MWCNTs) to generate a murine model of chronic granulomatous inflammation (6). Our previous studies have demonstrated that the MWCNT model shares characteristics with pulmonary sarcoidosis pathophysiology, including increased expression of proinflammatory mediators and decreased expression of alveolar macrophage ATP-binding cassette (ABC) lipid transporters, ABCA1 and ABCG1 (7, 8).

ABCA1 and ABCG1 facilitate the transfer of lipids across plasma membranes and play an important role in the catabolism of pulmonary surfactant. Deficiency of either ABCA1 or ABCG1 has been shown to promote pulmonary lipid accumulation (9, 10). Intracellular lipid accumulation has been shown to promote proinflammatory macrophage activation (11). Clinically, the deficiency of these lipid transporters has been observed in Tangier disease (ABCA1) and pulmonary alveolar proteinosis (ABCG1). These pathologies are characterized by dysregulated lipid homeostasis and elevated inflammatory mediators (12, 13). Upregulation of alveolar macrophage ABCG1 in a murine model of alveolar proteinosis has been shown to reduce pulmonary lipid accumulation and improve lung function (14).

These observations suggest that the lipid transporters, ABCA1 and ABCG1, may play a significant role in pulmonary granulomatous inflammation. To further address this hypothesis, we used myeloid-specific knockout (KO) mice, deficient in ABCA1, ABCG1, or both ABCA1 and ABCG1. We hypothesized that deficiency of the ABC-lipid transporters would exacerbate MWCNT-induced granulomatous inflammation.

## Methods

### Animals

Studies were conducted in accordance with the National Institutes of Health's Guide for the Care and Use of Laboratory Animals and approved by East Carolina University Institutional Animal Care and Use Committee. C57Bl/6J and myeloid-specific lipid transporter KO mice, generated by selectively crossing $Abca1^{flox/flox}Abcg1^{flox/flox}$ double-floxed mice (021067) with $LyzMCre^{+/+}$ (004781) mice, were obtained from Jackson Laboratory. Further information can be found in the data supplement. Animals were maintained under pathogen-free conditions. An equivalent number of both sexes was randomly assigned to experimental groups. Oropharyngeal instillation of MWCNTs or 35% surfactant (sham) was performed at 7 weeks of age, as previously described (6).

### Tissue Collection Quantitative Analysis of Tissue

Details provided in data supplement.

### RNA Purification and Analysis

Total RNA was collected using the miRNeasy Micro Kit (Qiagen) according to the manufacturer's protocol. Specific primers were obtained from Qiagen (data supplement). Quantitative PCR was performed on complimentary DNA synthesized with the RT2 First Strand Kit (Qiagen) and evaluated on the StepOnePlus PCR system (Thermo Fisher Scientific) in comparison to Gapdh using the $2^{-\Delta\Delta CT}$ method (15).

### Analysis of BAL Fluid

Cholesterol content was determined using the Amplex Red Cholesterol Assay kit (Thermo Fisher Scientific) according to the manufacturer's instructions in the presence of cholesterol esterase. The concentration of platelet-derived growth factor (PDGF) α and transforming growth factor (TGF)-β were determined using RayBio Mouse PDGF-AA ELISA Kit (cat. no. ELM-PDGFAA; RayBioTech) or LEGEND MAX Total TGF-β1 ELISA Kit (cat. no. 436707; BioLegend) according to the manufacturer's instructions.

### Phagocytosis Assay

Phagocytic ability of alveolar macrophages was evaluated using the pHrodo BioParticles Phagocytosis Flow Cytometry Kit (Thermo Fisher Scientific) according to manufacturer's protocol. The identification of alveolar macrophages was facilitated by counterstaining the cells with anti-CD11c. Alveolar macrophages were defined as $CD11c^{+}$ cells.

### Statistical Analysis

Data were analyzed by Student's *t* test (two groups) or two-way ANOVA (more than two groups), followed by Bonferroni correction using GraphPad Prism software (GraphPad Software). Significance was defined as a *P* value less than 0.05. Results shown are mean (±SEM).

## Results

### Macrophage ABCG1 Deficiency Promotes Pulmonary Granuloma Formation

To evaluate the effects of alveolar macrophage lipid transporter deficiency on pulmonary granuloma formation, myeloid-specific ABCA1, ABCG1, or ABCA1/ABCG1 double-KO (DKO) mice were used. Animals were evaluated 60 days after the instillation of 35% surfactant (sham) or 100 μg of MWCNT. Wild-type C57Bl/6J and ABCA1-KO sham-instilled animals were histologically indistinguishable (Figure 1). Sham-instilled ABCG1-KO or ABCA1/ABCG1-DKO animals, however, exhibited a marked increase of lipid-loaded alveolar macrophages within the airways (indicated by black arrows in Figure 1). These observations are similar to previous observations in ABCG1-deficient animals (10). After MWCNT instillation, pulmonary granulomas in C57Bl/6J and ABCA1-KO mice typically consisted of a compact carbon aggregate core surrounded by epithelioid macrophages, forming a smooth, discreet border to the granuloma (Figure 1). Granulomas in ABCG1-KO and ABCA1/ABCG1-DKO animals were markedly different, generally consisting of multiple, less compact carbon aggregates and irregular boarders of epithelioid macrophages (Figure 1). Representative images are shown in Figure 1.

Granulomatous inflammation was further characterized by determining the average number and size of MWCNT-induced lesions from digital images of hematoxylin and eosin–stained lung sections. Our analysis found no difference in the average number of granulomas per area of whole lung section between ABC-lipid transporter KOs and wild-type animals (Figure 2A). Evaluation of the mean granuloma area indicated no statistical difference between MWCNT-instilled ABCA1-KO and wild-type animals

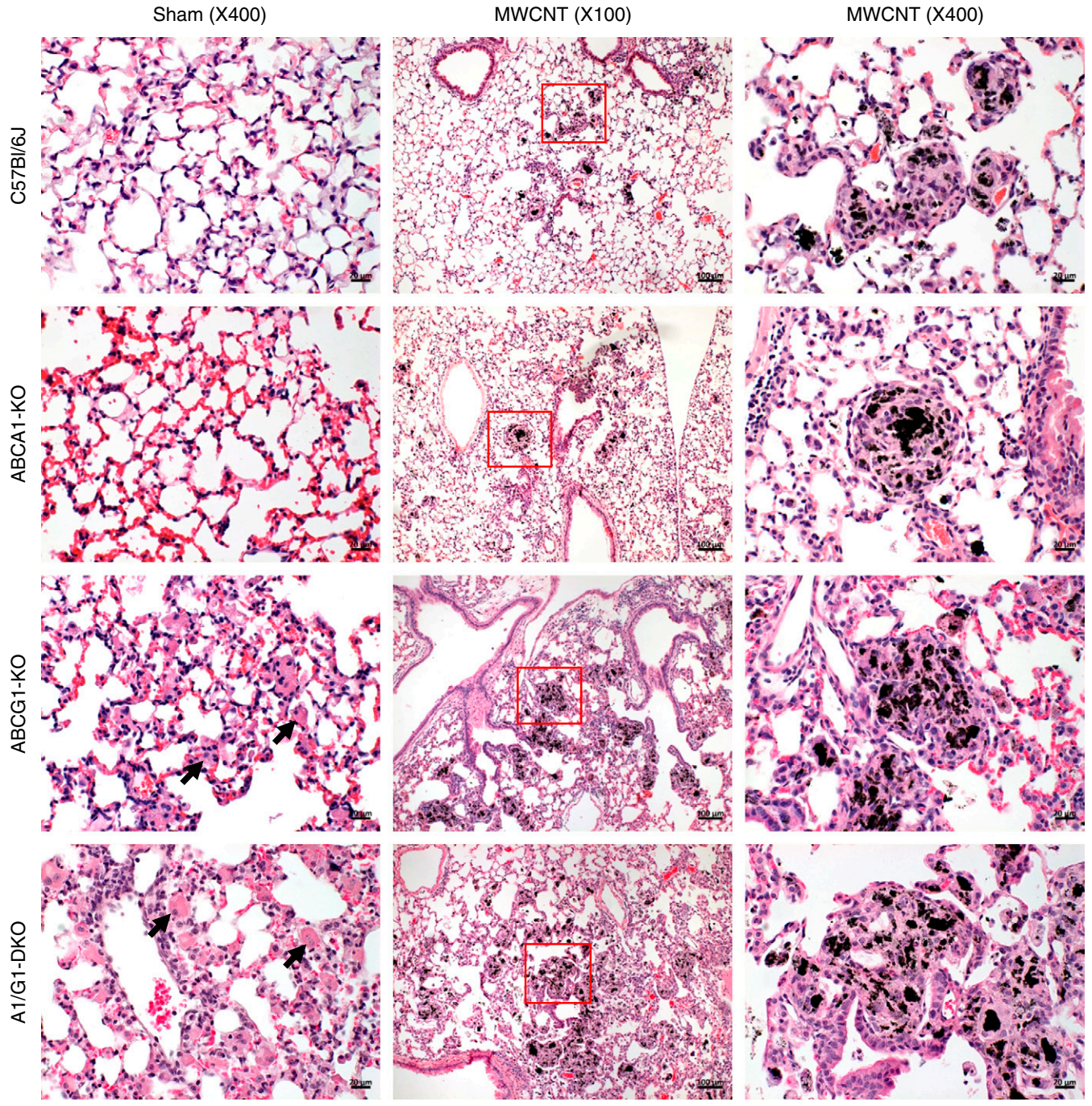


**Figure 1.** Multiwall carbon nanotube (MWCNT)-induced granuloma formation. Representative hematoxylin and eosin (H&E)–stained lung sections from C57Bl/6J and ATP-binding cassette (ABC) A1–knockout (KO), ABCG1-KO, and ABCA1/ABCG1 double-KO (DKO) sham-instilled animals (scale bars: 20 μm) or those receiving MWCNTs at low-power (scale bars: 100 μm) or high-power (scale bars: 20 μm) magnification. Lipid-loaded alveolar macrophages indicated by black arrows.

(Figure 2B). MWCNT-induced granulomas observed in ABCG1-KO and ABCA1/ABCG1-DKO animals, however, were found to be 35% and 39% larger, respectively, than those observed in wild-type animals (Figure 2B).

### Macrophage ABCG1 Deficiency Promotes Alveolar Macrophage Inflammatory Gene Expression

To determine if the BAL cell population was affected by MWCNTs, BAL was performed 60 days after MWCNT instillation. BALs from wild-type and ABCA1-KO BAL consisted of approximately $1.0 \times 10^6$ leukocytes, and were predominantly alveolar macrophages (>97%; *see* Figure E1 in the data supplement). ABCG1-KO and ABCA1/ABCG1-DKO BAL had twice as

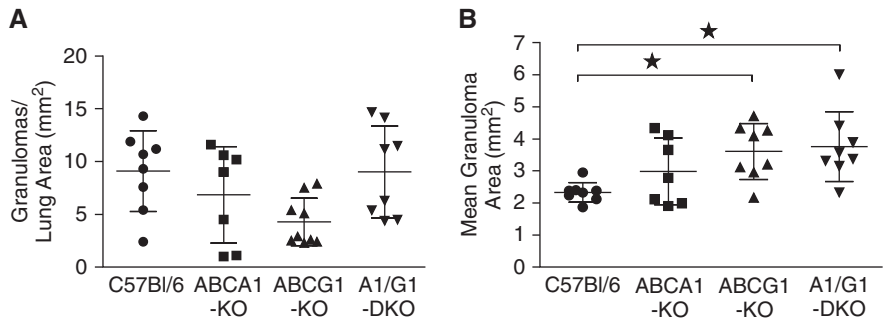


**Figure 2.** ABCG1 deficiency exacerbates the size of pulmonary granulomatous lesions. Pulmonary granuloma formation was quantified by evaluating the (*A*) number and (*B*) average size of MWCNT-induced lesions from H&E–stained lung tissue. Data represent mean ± SEM, $^{\star}P < 0.05$.

many isolated leukocytes ($\sim 2.0 \times 10^6$) compared with wild-type animals, and, as previously observed (16), included increased polymorphonuclear cells (9–16%; Figure E1). Neither the total cell count nor the composition of leukocytes in the lavage was affected by the instillation of MWCNTs compared with sham-instilled animals (Figure E1).

Previous studies have found that the proinflammatory mediators (C-C motif) ligand-2 (CCL2) and osteopontin play a critical role in the formation of pulmonary granulomas (17, 18). Our laboratory has reported the upregulation of these genes in BAL cells isolated from MWCNT-instilled, wild-type animals (19, 20). The data reported here are similar to those observations. The deficiency of ABCA1 did not promote CCL2 or osteopontin expression after MWCNT instillation (Figure 3). Sham-instilled ABCG1-KO animals exhibited significantly higher CCL2 and osteopontin expression compared with wild-type animals, and this increase was further exacerbated by the instillation of MWCNTs (Figure 3). Interestingly, BAL cells of sham-instilled ABCA1/ABCG1-DKO animals demonstrated significantly higher CCL2 and osteopontin expression than ABCG1-KO animals, but had no additional increase of these genes after MWCNT instillation (Figure 3).

### ABCG1 Deficiency Promotes MWCNT-induced Fibrosis and Profibrotic Mediators

The progression of pulmonary sarcoidosis is frequently characterized by the development of fibrosis. MWCNT-induced fibrosis was evaluated from whole lung sections after Gomori trichrome staining. We have previously reported that the MWCNT-induced granulomas of wild-type animals do not consistently demonstrate collagen deposition (6). Here, we sought to increase the sensitivity of our analysis by evaluating the entire lung. Using this method, we found that MWCNT-instilled wild-type animals have increased fibrosis when compared with sham-instilled animals (Figure 4A). MWCNT-instilled ABCA1-KO animals demonstrated a similar increase in fibrosis score compared with wild-type animals (Figure 4A). ABCG1-KO and ABCA1/ABCG1-DKO sham-instilled animals demonstrated a significantly higher fibrosis score than wild-type animals, and this increase was further exacerbated by the instillation of MWCNTs (Figure 4A). MWCNT-induced fibrosis in both ABCG1-KO and ABCA1/ABCG1-DKO animals was significantly greater than that observed in wild-type animals.

To further investigate the fibrotic changes, we evaluated alveolar macrophage gene expression and BAL fluid (BALF) protein concentration of the profibrotic mediators, PDGFα and TGF-β. We found that BAL cells from wild-type and ABCA1-KO animals demonstrated a similar increase in PDGFα expression after MWCNT instillation (Figure 4B). Sham-instilled ABCG1-KO and ABCA1/ABCG1-DKO BAL cells had significantly higher PDGFα mRNA expression than wild-type animals, and demonstrated a further increase after MWCNT instillation (Figure 4B). The combined deficiency of ABCA1/ABCG1 did not further promote BAL cell PDGFα expression. Evaluation of BAL cell TGF-β expression revealed no difference between wild-type and ABC-lipid transporter KO sham-instilled animals (Figure 4C). After MWCNT instillation, we observed a slight increase of TGF-β expression in BAL cells of ABCG1-KO (1.2 ± 0.2 fold) and ABCA1/ABCG1-DKO (1.2 ± 0.1 fold) animals compared with sham-instilled animals (Figure 4C). TGF-β expression did not statistically differ between MWCNT-instilled wild-type, ABCG1-KO, or ABCA1/ABCG1-DKO animals.

Further evaluation of BALF PDGFα protein concentration found no significant difference among sham-instilled wild-type (64.6 ± 13.2 pg/ml), ABCA1-KO (42.6 ± 10.2 pg/ml), ABCG1-KO (71.1 ± 7.2 pg/ml), or ABCA1/ABCG1-DKO (57.4 ± 2.0 pg/ml) animals. After MWCNT instillation, BALF PDGFα concentration was elevated in wild-type (104.6 ± 11.6 pg/ml, $P = 0.06$), ABCA1-KO (89.6 ± 8.9 pg/ml), ABCG1-KO (116.1 ± 8.1 pg/ml), and ABCA1/ABCG1-DKO (135.4 ± 20.3 pg/ml) animals (Figure 4D). BALF PDGFα protein concentration did not statistically differ between MWCNT-instilled wild-type and ABC-lipid transporter KO animals. BALF TGF-β protein concentrations of sham-instilled wild-type (31.0 ± 1.9 pg/ml) and ABCA1-KO (27.5 ± 1.8 pg/ml) animals were not statistically different.

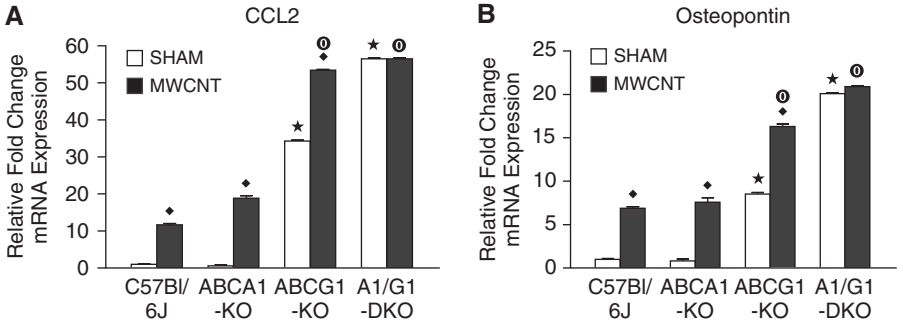


**Figure 3.** Macrophage ABCG1 deficiency promotes proinflammatory gene expression. Quantitative PCR analysis of (*A*) CCL2 and (*B*) osteopontin expression in BAL cells of sham- or MWCNT-instilled animals. $^{\star}P < 0.05$ C57Bl/6J-sham versus KO-sham, $^{\blacklozenge}P < 0.05$ sham versus MWCNT/strain, and $^{\circledcirc}P < 0.05$ C57Bl/6J-MWCNT versus KO-MWCNT. Data represent mean ± SEM, $n \geq 4$/treatment.

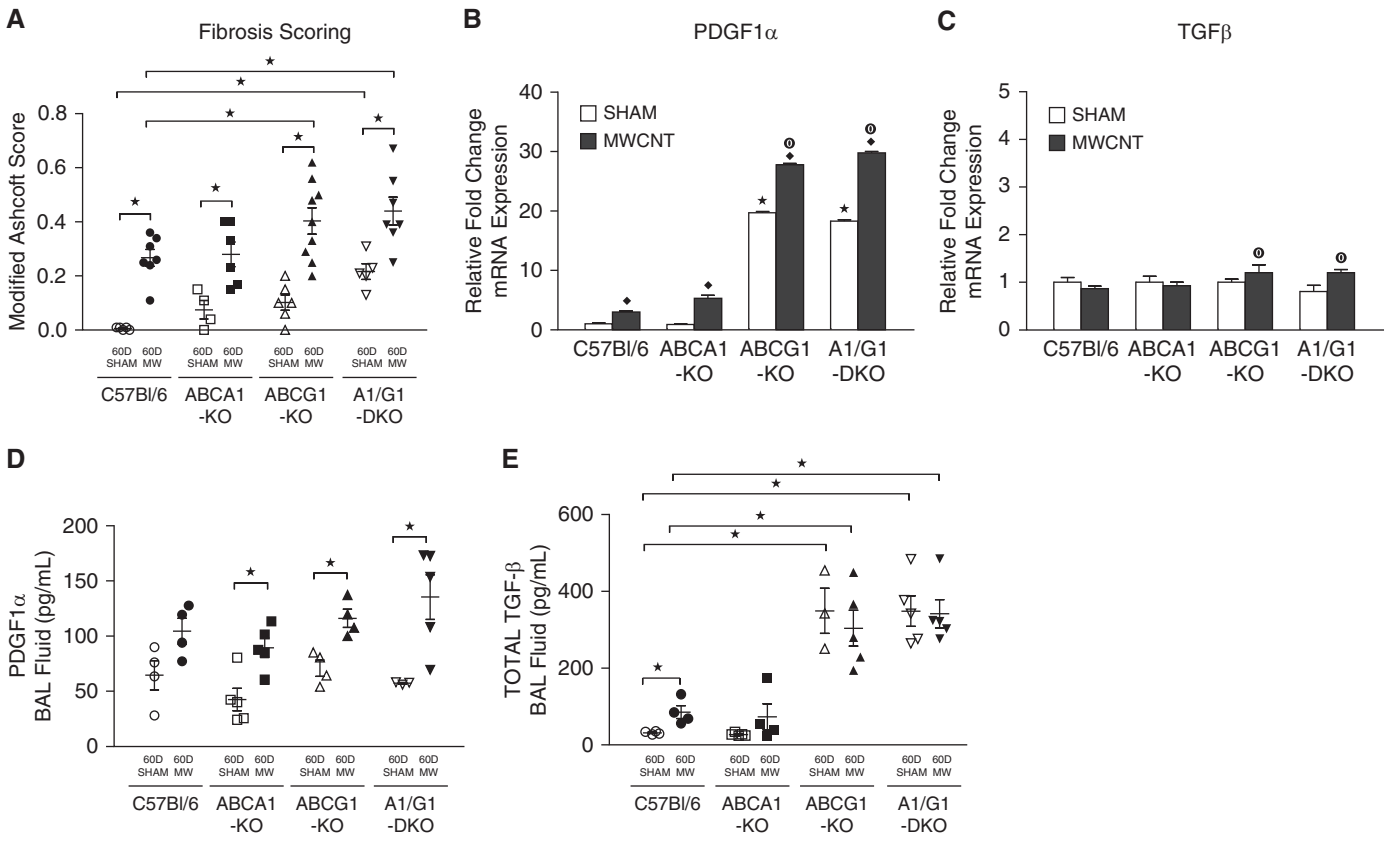


**Figure 4.** Deficiency of ABCG1 promotes pulmonary fibrosis. (*A*) Modified Ashcroft scoring of sham- or MWCNT-instilled, trichrome-stained whole-lung sections. Quantitative PCR analysis of (*B*) platelet-derived growth factor (PDGF) α and (*C*) transforming growth factor (TGF)-β expression in alveolar macrophages of sham- or MWCNT-instilled animals; $^{\star}P < 0.05$ C57Bl/6J-sham versus KO-sham, $^{\blacklozenge}P < 0.05$ sham versus MWCNT/strain, and $^{\circledast}P < 0.05$ C57Bl/6J-MWCNT versus KO-MWCNT, $n \geq 4$/treatment. The concentration of BAL fluid (BALF) (*C*) PDGFα and (*D*) total TGF-β in sham- and MWCNT-instilled animals; $^{\star}P < 0.05$. Data represent mean ± SEM. MW = MWCNT.

However, in contrast to BAL cell gene expression, TGF-β protein concentration of the BALF was significantly higher in ABCG1-KO (349.5 ± 58.9 pg/ml) and ABCA1/ABCG1-DKO (348.9 ± 39.7 pg/ml) animals when compared with wild-type mice (Figure 4E). After MWCNT instillation, we observed a slight increase of TGF-β protein concentration in wild-type (85.6 ± 16.6 pg/ml) and ABCA1-KO (73.1 ± 34.0 pg/ml) animals (Figure 4E). MWCNT-instilled ABCG1-KO (304.1 ± 46.6 pg/ml) and ABCA1/ABCG1-DKO (341.9 ± 36.7 pg/ml) animals demonstrated constitutively higher TGF-β protein content than wild-type animals, but were not statistically different from sham-instilled animals (Figure 4E).

### Instillation of MWCNTs Differentially Regulates the Expression of Lipid Transporters

The effects of MWCNT instillation were evaluated on the expression of the remaining lipid transporter in single-KO animals. ABCG1-mRNA was reduced in ABCA1-KO animals after MWCNT instillation, similar to changes observed in wild-type mice (8) (Figure 5A). In contrast, MWCNT instillation increased the expression of ABCA1-mRNA in ABCG1-KO animals (Figure 5B). Changes in pulmonary lipid composition were evaluated by measuring the total cholesterol content of the BALF. We found the BALF cholesterol concentration of sham-instilled wild-type (1.6 ± 0.1 μg/ml) and ABCA1-KO (1.5 ± 0.1 μg/ml) animals did not differ. However, ABCG1-KO (2.9 ± 0.3 μg/ml) and ABCA1/ABCG1-DKO (4.6 ± 0.6 μg/ml) animals showed progressive lipid accumulation in the lungs (Figure 5C). After MWCNT instillation, BALF cholesterol was significantly increased in wild-type (2.3 ± 0.2 μg/ml) and ABCA1-KO mice (2.4 ± 0.4 μg/ml). The increased BALF cholesterol content observed in ABCG1-KO (3.5 ± 0.3 μg/ml) and ABCA1/ABCG1-DKO (6.0 ± 1.0 μg/ml) mice failed to reach significance compared with sham-instilled animals, but was significantly greater than in MWCNT-instilled wild-type animals (Figure 5C).

Intracellular lipid accumulation was evaluated from Oil-Red-O (ORO)–stained whole-lung tissue of sham and MWCNT-instilled animals 60 days after instillation. Histological analysis was performed using a simplified scoring system taking into account the frequency of lipid-loaded macrophages throughout the tissue. Results indicate a slight increase of lipid-laden macrophages in sham-instilled ABCA1-KO (2.7 ± 0.3), ABCG1-KO (4.7 ± 0.3), and ABCA1/ABCG1-DKO (5.0 ± 0.1) animals compared with wild-type mice (1.3 ± 0.3). After MWCNT instillation, a slight but nonsignificant increase in ORO score was observed in wild-type animals (2.3 ± 0.2, $P = 0.07$). ORO score of MWCNT-instilled ABCA1-KO (2.3 ± 0.3), ABCG1-KO (4.3 ± 0.3), and ABCA1/ABCG1-DKO

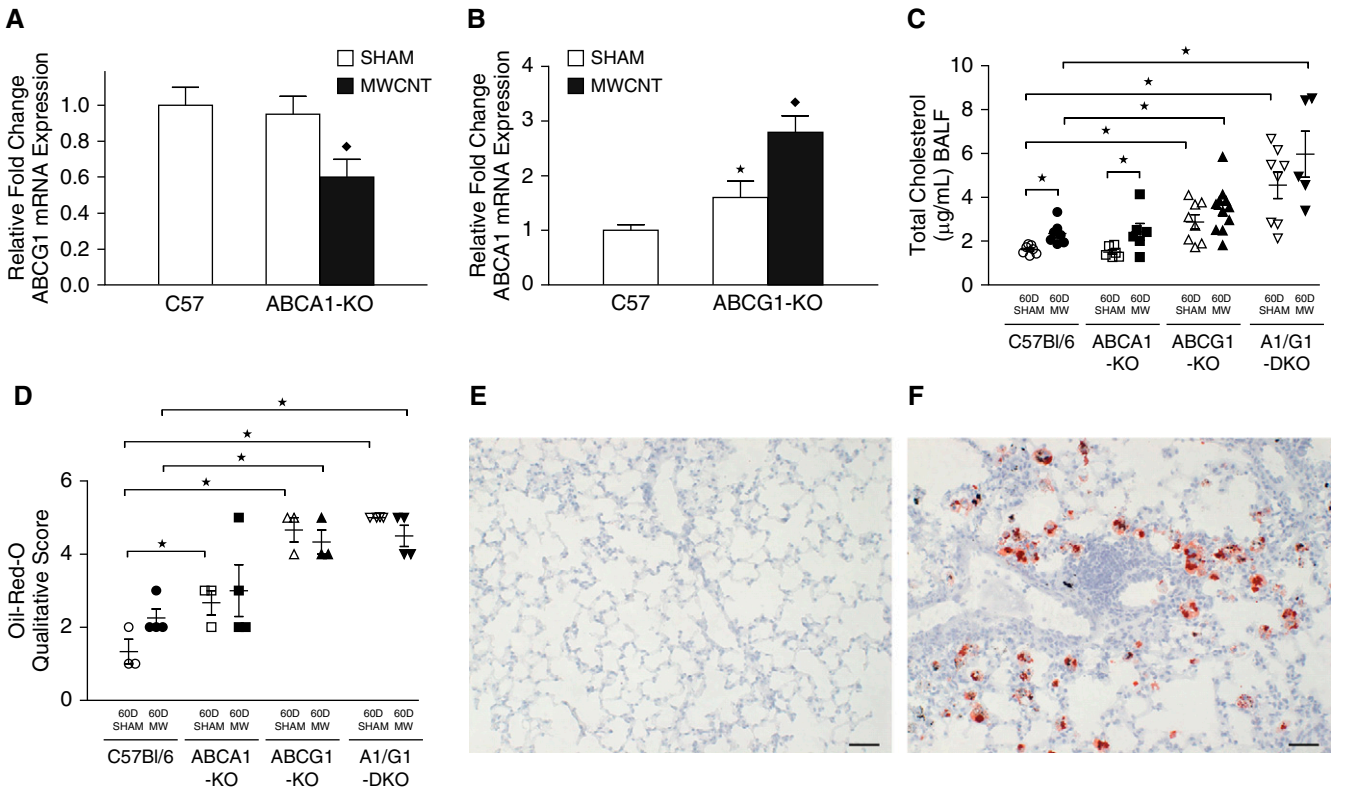


**Figure 5.** Instillation of MWCNTs affects ABC-lipid transporter expression and total cholesterol content of BALF. Quantitative PCR analysis of (*A*) ABCG1 expression in ABCA1-KO animals and (*B*) ABCA1 expression in ABCG1-KO animals; ★$P < 0.05$ C57Bl/6J-sham versus KO-sham, ♦$P < 0.05$ sham versus MWCNT/strain. (*C*) Total cholesterol content of BALF in sham- or MWCNT-instilled animals. (*D*) Qualitative analysis of Oil-Red-O (ORO)–stained lung tissue; ★$P < 0.05$. Representative images of (*E*) sham-instilled wild-type (1+) and (*F*) MWCNT-instilled ABCG1-KO (5+) scored ORO-stained lungs. Scale bars: 50 μm. Data represent mean ± SEM, $n \geq 4$/treatment.

(4.5 ± 0.3) animals did not statistically differ from vehicle instilled controls. ORO scores of MWCNT-instilled ABCG1-KO and ABCA1/ABCG1-DKO animals were statistically greater than scores of wild-type animals (Figure 5D). Representative images of sham-instilled wild-type (ORO 1+) and MWCNT-instilled ABCG1-KO (ORO 5+) animals are shown in Figures 5E and 5F, respectively.

### ABC-Lipid Transporter–Deficient Alveolar Macrophages Have Increased Carbon Content and Phagocytic Capacity

The observations that alveolar macrophage ABCG1 deficiency promotes MWCNT-induced granulomatous inflammation prompted us to further investigate how these cells phagocytose carbon nanoparticles. We hypothesized that ABCG1 deficiency would lead to a greater number of carbon-containing alveolar macrophages. To test this hypothesis, alveolar macrophages were evaluated from BAL cell cytospins for the presence or absence of intracellular carbon. We found that the percentages of alveolar macrophages containing carbon were significantly higher in each ABC-lipid transporter KO—ABCA1-KO (26 ± 3.4%), ABCG1-KO (22 ± 2.2%), and ABCA1/ABCG1-DKOs (22 ± 1.5%)—compared with wild-type (14 ± 1.4%) animals (Figure 6A). Although no significant difference was observed among ABCA1-KO, ABCG1-KO, and ABCA1/ABCG1-DKO animals, the increased percentage of ABCA1-KO macrophages containing carbon was unexpected.

To further define the phagocytic capacity of ABC-lipid transporter–deficient alveolar macrophages, BAL cells were incubated with pH-sensitive fluorescently labeled *Escherechia coli* particles and evaluated by flow cytometry. The percentage of alveolar macrophages that phagocytized labeled particles increased in ABCA1-KO (35 ± 1.9%) and, to a further extent, in ABCG1-KO (55 ± 2.5%) and ABCA1/ABCG1-DKO (51 ± 2.6%), compared with wild-type (24 ± 4.2%) animals (Figure 6B). Mean fluorescence intensity, a measure of the number of particles phagocytosed per macrophage, was significantly increased in ABCG1-KO and ABCA1/ABCG1-DKO animals, but not ABCA1-KO (Figure 6C). Representative contour plots of the percentage of alveolar macrophages that phagocytosed particles are shown in Figure 6D. These data are consistent with a previous report that found that ABCG1-deficient macrophages had an increased phagocytic capacity to clear apoptotic cells (16).

### MWCNT-induced Mediastinal Lymphadenopathy Is Exacerbated by the Deficiency of ABC-Lipid Transporters

Previous studies have shown the ability of intratracheally instilled MWCNTs to translocate to lung-associated lymph nodes (21). We sought to characterize the change

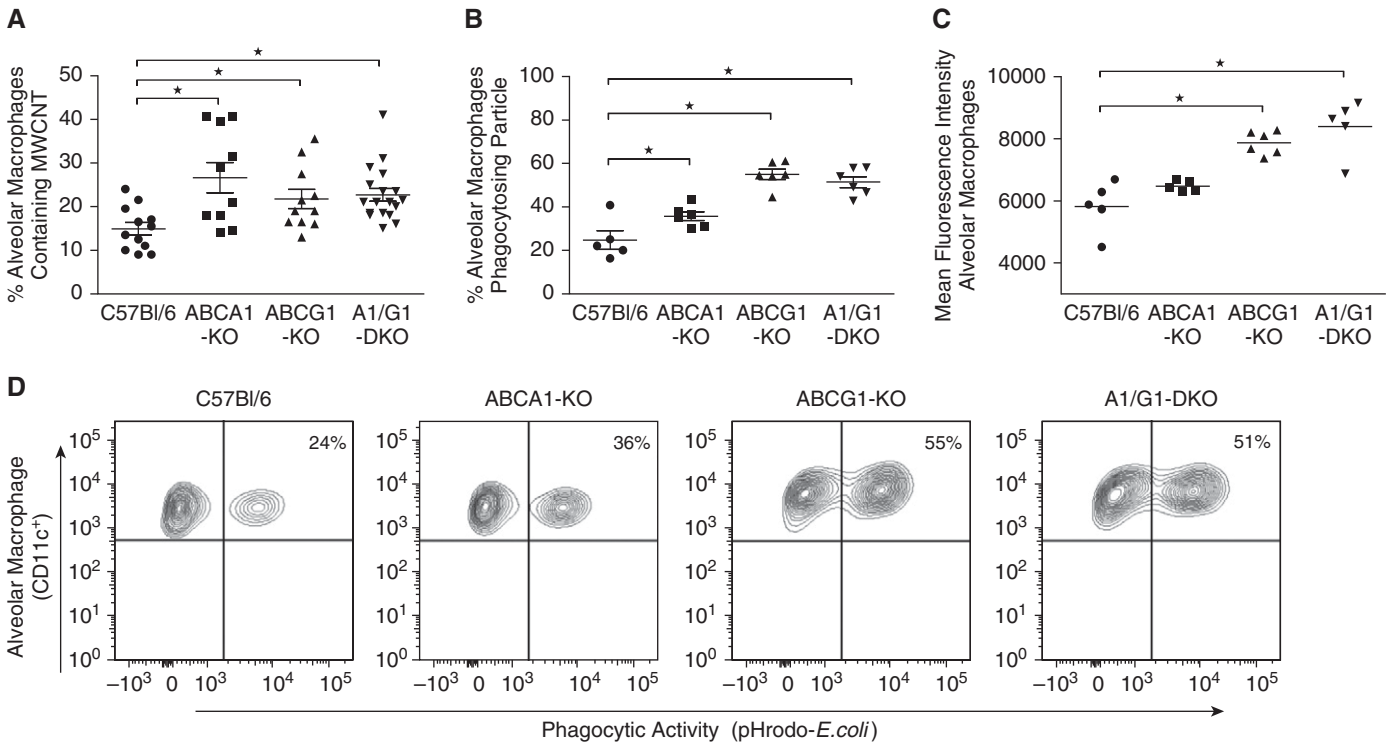


**Figure 6.** ABC-lipid transporter deficiency affects alveolar macrophage MWCNT content and phagocytic capacity. (*A*) Alveolar macrophages of C57Bl/6J or ABC-KO mice instilled with MWCNTs were visualized on BAL cell cytospins and evaluated for the presence of MWCNTs. The phagocytic capacity of alveolar macrophages isolated from naive animals was evaluated by determining the (*B*) percent of cells to phagocytose fluorescently labeled *Escherechia coli* particles and (*C*) mean florescence intensity per cell; ★$P < 0.05$. (*D*) Representative contour plots of the percent of alveolar macrophages phagocytosing *E. coli* particles. Data represent mean ± SEM.

in mediastinal lymph node volume in wild-type and ABC-lipid transporter–deficient animals after MWCNT instillation. The average mediastinal lymph node volume of sham-instilled wild-type (1.8 ± 0.2 $mm^3$) and ABCA1-KO (2.0 ± 0.2 $mm^3$) animals did not statistically differ; however, ABCG1-KO (6.6 ± 0.9 $mm^3$) and ABCA1/ABCG1-DKO (10.6 ± 1.2 $mm^3$) animals had a significant increase in lymph node volume. After MWCNT instillation, mediastinal lymph node volume was significantly increased in wild-type (4.8 ± 0.4 $mm^3$), ABCA1-KO (5.5 ± 0.7 $mm^3$), ABCG1-KO (9.7 ± 0.9 $mm^3$), and ABCA1/ABCG1-DKO (15.5 ± 1.2 $mm^3$) compared with sham-instilled mice. The MWCNT-induced mediastinal lymphadenopathy observed in ABCG1-KO and ABCA1/ABCG1-DKO mice was significantly greater than in wild-type animals (Figure 7A). Further evaluation found a significant correlation between mediastinal lymph node volume and the average size of MWCNT-induced pulmonary granulomas ($r = 0.68$, $P = 0.03$; Figure 7B), where paired data were available. Histological examination identified intracellular carbon deposition throughout the lymph nodes, but no evidence of granuloma formation in MWCNT-instilled animals (images not shown).

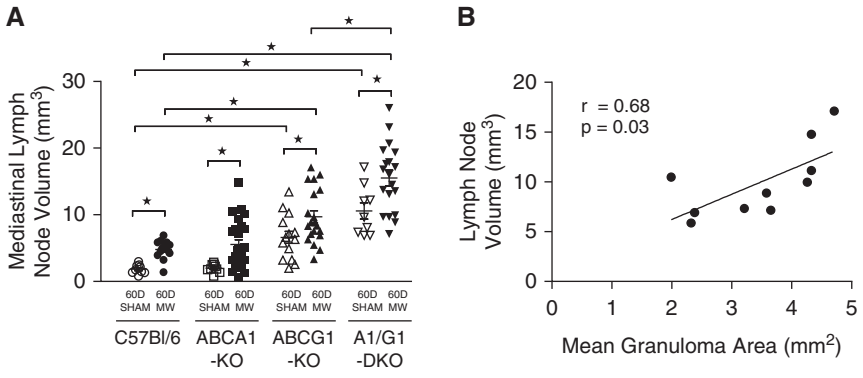


**Figure 7.** MWCNT-induced lymphadenopathy is exacerbated by the deficiency of ABCG1. (*A*) Tracheobronchial lymph node volume was determined from sham- or MWCNT-instilled animals; ★$P < 0.02$. Data represent mean ± SEM. (*B*) Correlation was determined for animals with paired mediastinal lymph node volume and mean granuloma area.

## Discussion

We have previously described an MWCNT-induced model of chronic granulomatous inflammation, which bears striking similarity to pulmonary sarcoidosis, including the deficiency of alveolar macrophage lipid transporters, ABCA1 and ABCG1 (6, 8). The deficiency of these genes correlates with pulmonary lipid accumulation and increased expression of

proinflammatory mediators in the MWCNT model (7, 8). Although the deficiency of ABCA1 or ABCG1 has been shown to promote pulmonary lipid accumulation (9, 22), the involvement of these transporters in chronic granulomatous lung disease remains unclear. We aimed to determine if the deficiency of alveolar macrophage ABCA1 or ABCG1 contributes to pulmonary granuloma formation and inflammation. Here, we report that deficiency of alveolar macrophage ABCG1, but not ABCA1, promotes MWCNT-induced pulmonary granuloma size, pulmonary fibrosis, profibrotic mediators, and the expression of CCL2 and osteopontin. These observations correlate with the dysregulation of pulmonary lipid homeostasis, and suggest that alveolar macrophage ABCG1 acts as a negative regulator of pulmonary granulomatous inflammation.

The proinflammatory mediators, CCL2 and osteopontin, are upregulated in granulomatous tissue of patients with pulmonary sarcoidosis and wild-type animals bearing MWCNT-induced granulomas (19, 23–25). Deficiency of these genes in murine studies prevents the formation of pulmonary granulomas in response to stimuli (17, 18), suggesting that these mediators play an integral role in the process. ABCG1 deficiency has been shown to promote pulmonary inflammation, including increased expression of CCL2 in lung tissue of total KO animals (26). To our knowledge, the expression of osteopontin has not been evaluated in the lungs of lipid transporter–deficient mice. Evaluation of CCL2 and osteopontin found intrinsic elevation of these mediators in alveolar macrophages deficient in ABCG1 and further upregulation after MWCNT instillation. The increased expression of these mediators in ABCG1 or ABCA1/ABCG1 myeloid-specific KO animals likely promotes MWCNT-induced granuloma formation.

Here, we report that deficiency of alveolar macrophage ABCG1 or the combined deficiency of ABCA1/ABCG1 promotes MWCNT-induced pulmonary fibrosis and the profibrotic mediators, PDGFα and TGF-β. These observations correlate with the progressive pulmonary lipid accumulation noted in these animals. Previous studies have reported lipid-loaded macrophages in patients suffering from fibrotic lung disease and in animal models of pulmonary fibrosis (27–30). Romero and colleagues (31) demonstrated that deficiency of ABCG1, in part due to pulmonary lipid accumulation, promotes bleomycin-induced lung fibrosis. Interestingly, transcriptome analysis of lipid-loaded macrophages isolated from a subcutaneous granuloma model exhibited upregulation of profibrotic pathways (32). These observations support a link between dysregulated pulmonary lipid homeostasis and the progression of lung diseases.

In an effort to better describe how ABC-lipid transporter–deficient alveolar macrophages respond to carbon nanoparticles, we evaluated the carbon content and phagocytic capacity of these cells. We found an increased number of carbon-containing alveolar macrophages in ABCA1-KO, ABCG1-KO, and ABCA1/ABCG1-DKO mice when compared with wild-type animals. Further studies demonstrated that the phagocytic ability of these cells increases in the order of: *ABCA1/ABCG1-DKO* $\approx$ *ABCG1-KO* $>$ *ABCA1-KO* $>$ *C57Bl/6J (wild-type)*. The increased number of carbon-laden macrophages in ABCA1-KO BAL was unexpected. Given the increased total BAL cell count observed in the ABCG1 and ABCA1/ABCG1-DKO animals, it may be inferred that the macrophage:carbon ratio is decreased in these animals, explaining the relatively equal number of carbon-containing macrophages in ABCA1-KO animals. Although these studies do not account for the distinct mechanisms of *E. coli* and carbon nanotube phagocytosis, the observation suggests that macrophage deficiency of ABCG1 or combined deficiency of ABCA1/ABCG1 promotes carbon nanotube phagocytosis and retention in the lung, increasing pulmonary toxicity and inflammation.

Mediastinal and hilar lymph node involvement are defining characteristics of the initial stages of pulmonary sarcoidosis. These data demonstrate that the deficiency of macrophage ABCG1 exacerbates mediastinal lymphadenopathy in both check sham- and MWCNT-instilled animals. This observation may reflect the proinflammatory phenotype that characterizes the lungs of ABCG1- and ABCA1/ABCG1–deficient animals. Despite the presence of MWCNTs in the lymph nodes, no granulomas were observed. This finding may reflect absence of an immunologic antigen or the time point evaluated, 60 days after instillation. Carbon nanotubes have been shown to accumulate in the lymph nodes over time (21), and our laboratory has made similar observations in the MWCNT model. Interestingly, a significant positive correlation was found between mediastinal lymph node volume and the average size of pulmonary granulomas, a relationship that warrants further investigation.

An unexpected observation made during the course of these studies was the absence of a significant increase in proinflammatory mediators in ABCA1-KO mice. Previous reports have found progressive pulmonary lipid accumulation in complete ABCA1-KO animals (9, 33), but at a slower rate than observed in ABCG1-deficient animals. The absence of significant pulmonary lipid accumulation may explain the lack of an inflammatory phenotype. Previous studies have also indicated that the inflammatory potential of ABCA1-deficient macrophages is less than those deficient in ABCG1 or ABCA1/ABCG1. After LPS stimulation, peritoneal macrophages of ABCA1-deficient animals demonstrated only a slight increase in a limited subset of inflammatory cytokines compared with ABCG1 or, to a greater extent, ABCA1/ABCG1-DKO peritoneal macrophages (11).

The progressive stages of pulmonary sarcoidosis are characterized by hilar node involvement, granulomatous infiltrates into the lungs, and end-stage pulmonary fibrosis (34). Here, we demonstrate that the deficiency of alveolar macrophage ABCG1 exacerbates each of these clinical parameters in response to the instillation of carbon nanotubes. Recently, we have reported that upregulation of alveolar macrophage ABCG1 expression and inhibition of pulmonary lipid accumulation correlate with reduced MWCNT-induced pulmonary granuloma formation and proinflammatory macrophage activation (35). These observations, together with those presented in the current study, demonstrate that alveolar macrophage ABCG1 is a crucial regulator of pulmonary granuloma formation and inflammation. ■

**Author disclosures** are available with the text of this article at www.atsjournals.org.

**Acknowledgment:** The authors thank ONY Biotech for kindly providing surfactant for use in these studies.

## References


1. Baughman RP, Teirstein AS, Judson MA, Rossman MD, Yeager H Jr, Bresnitz EA, *et al*.; Case Control Etiologic Study of Sarcoidosis (ACCESS) Research Group. Clinical characteristics of patients in a case control study of sarcoidosis. *Am J Respir Crit Care Med* 2001;164:1885–1889.
2. Kajdasz DK, Lackland DT, Mohr LC, Judson MA. A current assessment of rurally linked exposures as potential risk factors for sarcoidosis. *Ann Epidemiol* 2001;11:111–117.
3. Kreider ME, Christie JD, Thompson B, Newman L, Rose C, Barnard J, *et al*. Relationship of environmental exposures to the clinical phenotype of sarcoidosis. *Chest* 2005;128:207–215.
4. Prezant DJ, Dhala A, Goldstein A, Janus D, Ortiz F, Aldrich TK, *et al*. The incidence, prevalence, and severity of sarcoidosis in New York City firefighters. *Chest* 1999;116:1183–1193.
5. Lam CW, James JT, McCluskey R, Hunter RL. Pulmonary toxicity of single-wall carbon nanotubes in mice 7 and 90 days after intratracheal instillation. *Toxicol Sci* 2004;77:126–134.
6. Huizar I, Malur A, Midgette YA, Kukoly C, Chen P, Ke PC, *et al*. Novel murine model of chronic granulomatous lung inflammation elicited by carbon nanotubes. *Am J Respir Cell Mol Biol* 2011;45:858–866.
7. Barna BP, Judson MA, Thomassen MJ. Carbon nanotubes and chronic granulomatous disease. *Nanomaterials (Basel)* 2014;4:508–521.
8. Barna BP, McPeek M, Malur A, Fessler MB, Wingard CJ, Dobbs L, *et al*. Elevated microRNA-33 in sarcoidosis and a carbon nanotube model of chronic granulomatous disease. *Am J Respir Cell Mol Biol* 2016;54: 865–871.
9. Bates SR, Tao JQ, Collins HL, Francone OL, Rothblat GH. Pulmonary abnormalities due to ABCA1 deficiency in mice. *Am J Physiol Lung Cell Mol Physiol* 2005;289:L980–L989.
10. Baldán A, Tarr P, Vales CS, Frank J, Shimotake TK, Hawgood S, *et al*. Deletion of the transmembrane transporter ABCG1 results in progressive pulmonary lipidosis. *J Biol Chem* 2006;281:29401–29410.
11. Yvan-Charvet L, Welch C, Pagler TA, Ranalletta M, Lamkanfi M, Han S, *et al*. Increased inflammatory gene expression in ABC transporter-deficient macrophages: free cholesterol accumulation, increased signaling via Toll-like receptors, and neutrophil infiltration of atherosclerotic lesions. *Circulation* 2008;118:1837–1847.
12. Bochem AE, van der Valk FM, Tolani S, Stroes ES, Westerterp M, Tall AR. Increased systemic and plaque inflammation in ABCA1 mutation carriers with attenuation by statins. *Arterioscler Thromb Vasc Biol* 2015;35:1663–1669.
13. Thomassen MJ, Barna BP, Malur AG, Bonfield TL, Farver CF, Malur A, *et al*. ABCG1 is deficient in alveolar macrophages of GM-CSF knockout mice and patients with pulmonary alveolar proteinosis. *J Lipid Res* 2007;48:2762–2768.
14. Malur A, Huizar I, Wells G, Barna BP, Malur AG, Thomassen MJ. Lentivirus-ABCG1 instillation reduces lipid accumulation and improves lung compliance in GM-CSF knock-out mice. *Biochem Biophys Res Commun* 2011;415:288–293.
15. Livak KJ, Schmittgen TD. Analysis of relative gene expression data using real-time quantitative PCR and the 2(-Delta Delta C(T)) method. *Methods* 2001;25:402–408.
16. Wojcik AJ, Skaflen MD, Srinivasan S, Hedrick CC. A critical role for ABCG1 in macrophage inflammation and lung homeostasis. *J Immunol* 2008;180:4273–4282.
17. Lu B, Rutledge BJ, Gu L, Fiorillo J, Lukacs NW, Kunkel SL, *et al*. Abnormalities in monocyte recruitment and cytokine expression in monocyte chemoattractant protein 1–deficient mice. *J Exp Med* 1998;187:601–608.
18. O'Regan AW, Hayden JM, Body S, Liaw L, Mulligan N, Goetschkes M, *et al*. Abnormal pulmonary granuloma formation in osteopontin-deficient mice. *Am J Respir Crit Care Med* 2001;164:2243–2247.
19. Huizar I, Malur A, Patel J, McPeek M, Dobbs L, Wingard C, *et al*. The role of PPARγ in carbon nanotube-elicited granulomatous lung inflammation. *Respir Res* 2013;14:7.
20. Malur A, Barna BP, Patel J, McPeek M, Wingard CJ, Dobbs L, *et al*. Exposure to a mycobacterial antigen, ESAT-6, exacerbates granulomatous and fibrotic changes in a multiwall carbon nanotube model of chronic pulmonary disease. *J Nanomed Nanotechnol* 2015; 6:340.
21. Aiso S, Kubota H, Umeda Y, Kasai T, Takaya M, Yamazaki K, *et al*. Translocation of intratracheally instilled multiwall carbon nanotubes to lung-associated lymph nodes in rats. *Ind Health* 2011;49:215–220.
22. Baldán A, Tarr P, Lee R, Edwards PA. ATP-binding cassette transporter G1 and lipid homeostasis. *Curr Opin Lipidol* 2006;17:227–232.
23. O'Regan AW, Chupp GL, Lowry JA, Goetschkes M, Mulligan N, Berman JS. Osteopontin is associated with T cells in sarcoid granulomas and has T cell adhesive and cytokine-like properties in vitro. *J Immunol* 1999;162:1024–1031.
24. Palchevskiy V, Hashemi N, Weigt SS, Xue YY, Derhovanessian A, Keane MP, *et al*. Immune response CC chemokines CCL2 and CCL5 are associated with pulmonary sarcoidosis. *Fibrogenesis Tissue Repair* 2011;4:10.
25. Barna BP, Huizar I, Malur A, McPeek M, Marshall I, Jacob M, *et al*. Carbon nanotube–induced pulmonary granulomatous disease: twist1 and alveolar macrophage M1 activation. *Int J Mol Sci* 2013;14: 23858–23871.
26. Baldán A, Gomes AV, Ping P, Edwards PA. Loss of ABCG1 results in chronic pulmonary inflammation. *J Immunol* 2008;180:3560–3568.
27. Basset-Léobon C, Lacoste-Collin L, Aziza J, Bes JC, Jozan S, Courtade-Saïdi M. Cut-off values and significance of Oil Red O–positive cells in bronchoalveolar lavage fluid. *Cytopathology* 2010; 21:245–250.
28. Hayes D Jr, Kirkby S, S McCoy K, Mansour HM, Khosravi M, Strawbridge H, *et al*. Reduction of lipid-laden macrophage index after laparoscopic Nissen fundoplication in cystic fibrosis patients after lung transplantation. *Clin Transplant* 2013;27:121–125.
29. Yasuda K, Sato A, Nishimura K, Chida K, Hayakawa H. Phospholipid analysis of alveolar macrophages and bronchoalveolar lavage fluid following bleomycin administration to rabbits. *Hai* 1994;172:91–102.
30. Azuma A, Li YJ, Abe S, Usuki J, Matsuda K, Henmi S, *et al*. Interferon-β inhibits bleomycin-induced lung fibrosis by decreasing transforming growth factor-β and thrombospondin. *Am J Respir Cell Mol Biol* 2005;32:93–98.
31. Romero F, Shah D, Duong M, Penn RB, Fessler MB, Madenspacher J, *et al*. A pneumocyte-macrophage paracrine lipid axis drives the lung toward fibrosis. *Am J Respir Cell Mol Biol* 2015;53:74–86.
32. Thomas AC, Eijgelaar WJ, Daemen MJ, Newby AC. Foam cell formation in vivo converts macrophages to a pro-fibrotic phenotype. *PLoS One* 2015;10:e0128163.
33. McNeish J, Aiello RJ, Guyot D, Turi T, Gabel C, Aldinger C, *et al*. High density lipoprotein deficiency and foam cell accumulation in mice with targeted disruption of ATP-binding cassette transporter-1. *Proc Natl Acad Sci USA* 2000;97:4245–4250.
34. Wessendorf TE, Bonella F, Costabel U. Diagnosis of sarcoidosis. *Clin Rev Allergy Immunol* 2015;49:54–62.
35. McPeek M, Malur A, Tokarz DA, Murray G, Barna BP, Thomassen MJ. PPAR-gamma pathways attenuate pulmonary granuloma formation in a carbon nanotube induced murine model of sarcoidosis. *Biochem Biophys Res Commun* 2018;503:684–690.